The EMBO Journal (2005) 24, 2873–2884 | © 2005 European Molecular Biology Organization | All Rights Reserved 0261-4189/05
www.embojournal.org

THE EMBO JOURNAL

Interactions between NEEP21, GRIP1 and GluR2 regulate sorting and recycling of the glutamate receptor subunit GluR2

Pascal Steiner[1,4], Stefano Alberi[2], Karina Kulangara[1], Alexandre Yersin[1], Juan-Carlos Floyd Sarria[1], Etienne Regulier[1], Sandor Kasas[1], Giovanni Dietler[3], Dominique Muller[2], Stefan Catsicas[1] and Harald Hirling[1,*]

[1]Brain Mind Institute, Faculté des Sciences de la Vie, Ecole Polytechnique Fédérale de Lausanne, Lausanne, Switzerland, [2]Département des Neurosciences Fondamentales, Centre Médical Universitaire, Université de Genève, Geneva, Switzerland and [3]Faculté des Sciences de Base, Ecole Polytechnique Fédérale de Lausanne, Lausanne, Switzerland

Trafficking of AMPA-type glutamate receptors (AMPAR) between endosomes and the postsynaptic plasma membrane of neurons plays a central role in the control of synaptic strength associated with learning and memory. The molecular mechanisms of its regulation remain poorly understood, however. Here we show by biochemical and atomic force microscopy analyses that NEEP21, a neuronal endosomal protein necessary for receptor recycling including AMPAR, is associated with the scaffolding protein GRIP1 and the AMPAR subunit GluR2. Moreover, the interaction between NEEP21 and GRIP1 is regulated by neuronal activity. Expression of a NEEP21 fragment containing the GRIP1-binding site decreases surface GluR2 levels and delays recycling of internalized GluR2, which accumulates in early endosomes and lysosomes. Infusion of this fragment into pyramidal neurons of hippocampal slices induces inward rectification of AMPAR-mediated synaptic responses, suggesting decreased GluR2 expression at synapses. These results indicate that NEEP21–GRIP1 binding is crucial for GluR2-AMPAR sorting through endosomes and their recruitment to the plasma membrane, providing a first molecular mechanism to differentially regulate AMPAR subunit cycling in internal compartments.

The EMBO Journal (2005) **24,** 2873–2884. doi:10.1038/sj.emboj.7600755; Published online 21 July 2005
Subject Categories: membranes & transport; neuroscience
Keywords: AMPAR; endosomes; neurons; recycling; synaptic plasticity

*Corresponding author. School of Life Sciences, Swiss Federal Institute of Technology, 1015 Lausanne, Switzerland. Tel.: +41 21 693 5363; Fax: +41 21 693 9538; E-mail: harald.hirling@epfl.ch
[4]Present address: Department of Neurobiology, Harvard Medical School, 220 Longwood Avenue, Boston, MA 02115, USA

Received: 24 February 2005; accepted: 30 June 2005; published online: 21 July 2005

Introduction

The number of AMPA-type glutamate receptors at the synaptic surface is regulated by endocytosis on the one hand, and recycling and exocytosis on the other hand, which is a major determinant of synaptic strength (Barry and Ziff, 2002; Malinow and Malenka, 2002; Sheng and Kim, 2002; Song and Huganir, 2002; Bredt and Nicoll, 2003). Induction of long-term depression (LTD) in hippocampal neuron cultures, hippocampal slice preparations and cultured cerebellar Purkinje cells is associated with a decrease in cell surface AMPA-type glutamate receptors (AMPAR) (Luscher *et al*, 1999; Beattie *et al*, 2000; Man *et al*, 2000; Matsuda *et al*, 2000; Xia *et al*, 2000). Likewise, during induction of long-term potentiation (LTP), AMPAR are recruited into synapses (Shi *et al*, 1999; Lu *et al*, 2001). The involvement of AMPAR trafficking in synaptic plasticity was also confirmed *in vivo* (Heynen *et al*, 2003; Lu *et al*, 2003; Takahashi *et al*, 2003). Despite the importance of this trafficking for synaptic transmission and plasticity, the molecular mechanisms involved, particularly at the level of the intracellular sorting compartments, are still poorly understood.

AMPAR are hetero-oligomers composed of the subunits GluR1–4, and GluR1/2 and GluR2/3 receptors are predominant in the hippocampus. AMPAR containing edited GluR2 are Ca^{2+}-impermeable, and the appearance of Ca^{2+}-permeable, GluR2-lacking receptors was linked to transient forebrain ischemia (Pellegrini-Giampietro *et al*, 1997; Liu *et al*, 2004). In hippocampal slice cultures, GFP-GluR1 is delivered to the synaptic surface in an activity-dependent manner (Shi *et al*, 1999), which is proposed to be the initial event to increase the number of surface AMPAR upon LTP induction. Unlike GluR1/2-AMPAR, GluR2/3-AMPAR cycle rapidly and constitutively between the synaptic surface and intracellular endosomes (Passafaro *et al*, 2001; Shi *et al*, 2001). The constitutive GluR2/3 cycling is believed to replace the newly inserted GluR1/2 receptors, thereby stabilizing the LTP-induced increase in surface receptor number (Shi *et al*, 2001). Following internalization in hippocampal neuron cultures, AMPAR can be differentially sorted by an unknown mechanism. Upon incubation with AMPA/tetrodotoxin (TTX) or NMDA, they are sent to lysosomal degradation, while following stimulation with AMPA or NMDA/TTX they recycle back to the plasma membrane (Ehlers, 2000; Lee *et al*, 2004).

GluR1 and GluR4 differ from GluR2 and GluR3 in their cytoplasmic tails. These tails determine subunit-specific trafficking, because they bind specific subsets of proteins. While the carboxy termini of GluR1 and GluR4 bind type I PDZ (postsynaptic density 95/disc large/zonula occludens-1), proteins like SAP97, GluR2 and GluR3 mainly interact with the type II PDZ proteins PICK1, GRIP1 and ABP (Barry and Ziff, 2002; Malinow and Malenka, 2002; Sheng and Kim, 2002; Song and Huganir, 2002; Bredt and Nicoll, 2003). GluR2 mutants, which show unaffected PICK1 binding but

abolished GRIP1 binding, indicate an essential role of GRIP1 in stabilization of AMPAR at the synapse (Chung *et al*, 2000; Matsuda *et al*, 2000; Xia *et al*, 2000). In addition to GRIP1 localized at the plasma membrane, a significant portion is also detected on internal compartments (Dong *et al*, 1997; Daw *et al*, 2000; Braithwaite *et al*, 2002), which might be involved in regulating the recruitment of AMPAR from intracellular storage organelles to the synaptic surface (Collingridge and Isaac, 2003). In non-neuronal cells, recycling receptors pass first through early endosomes, and then through tubular recycling endosomes, although their sorting along these compartments is not yet clear (Maxfield and McGraw, 2004). Internalized AMPAR have been colocalized with the endosomal SNARE trafficking protein syntaxin 13 (Lin *et al*, 2000) and the small GTPase Rab4 (Ehlers, 2000).

We have recently identified NEEP21, an early endosomal protein primarily detected in the somatodendritic compartment of neurons, which is immunoprecipitated with syntaxin 13 (Steiner *et al*, 2002). We demonstrated that suppression of NEEP21 leads to impaired recycling of internalized transferrin (Tf) receptor (TfR) (Steiner *et al*, 2002) and neurotension receptor 2 (Debaigt *et al*, 2004). This indicated that NEEP21 is an essential component for receptor sorting and recycling. Strikingly, NEEP21 suppression led to strong retardation of GluR1 and GluR2 recycling following NMDA/TTX-induced internalization. In the present study, we show that NEEP21 forms a complex with GRIP1 and GluR2. Disruption of NEEP21–GRIP1 binding has drastic effects on GluR2, but not GluR1, cycling, and causes inward rectification of AMPAR-mediated synaptic responses. These results strongly indicate that NEEP21 regulates endosomal sorting of AMPAR and excitatory neurotransmission by virtue of its direct interaction with GRIP1–GluR2.

Results

NEEP21 forms a regulated complex with GRIP1 and GluR2

We have previously shown that suppression of NEEP21 strongly delays recycling of internalized surface receptors, including the AMPAR subunits GluR1 and GluR2 in hippocampal neurons (Steiner *et al*, 2002). In order to verify this result by an independent approach, we overexpressed in hippocampal neurons either GFP or GFP fused to the entire cytosolic domain of NEEP21 spanning amino acids (aa) 104–185 (GFP-N104–185). We noticed that GFP-N104–185-transfected neurons had shorter dendrites. We analyzed internalization and recycling of GluR1 and GluR2 following TTX preincubation and NMDA stimulation, by immunolabeling for surface GluR1 and GluR2 (Steiner *et al*, 2002). At steady state, there was a modest, but significant reduction in surface labeling for GluR1 (Figure 1A) and GluR2 (Figure 1B). Following stimulation, GluR1 and GluR2 decreased at the neuronal surface in the presence of GFP or GFP-N104–185, reflecting receptor internalization. At 60 min, reappearance of both GluR1 and GluR2 was strongly impaired by GFP-N104–185 compared to control GFP. In order to distinguish cycling of GluR1 and GluR2 receptors, we also analyzed surface appearance of transfected HA-tagged GluR1 or GluR2. In contrast to endogenous heteromeric AMPAR, exogenously expressed GluR1 or GluR2 form homomeric receptors (Shi *et al*, 1999, 2001). As for the endogenous receptors, the

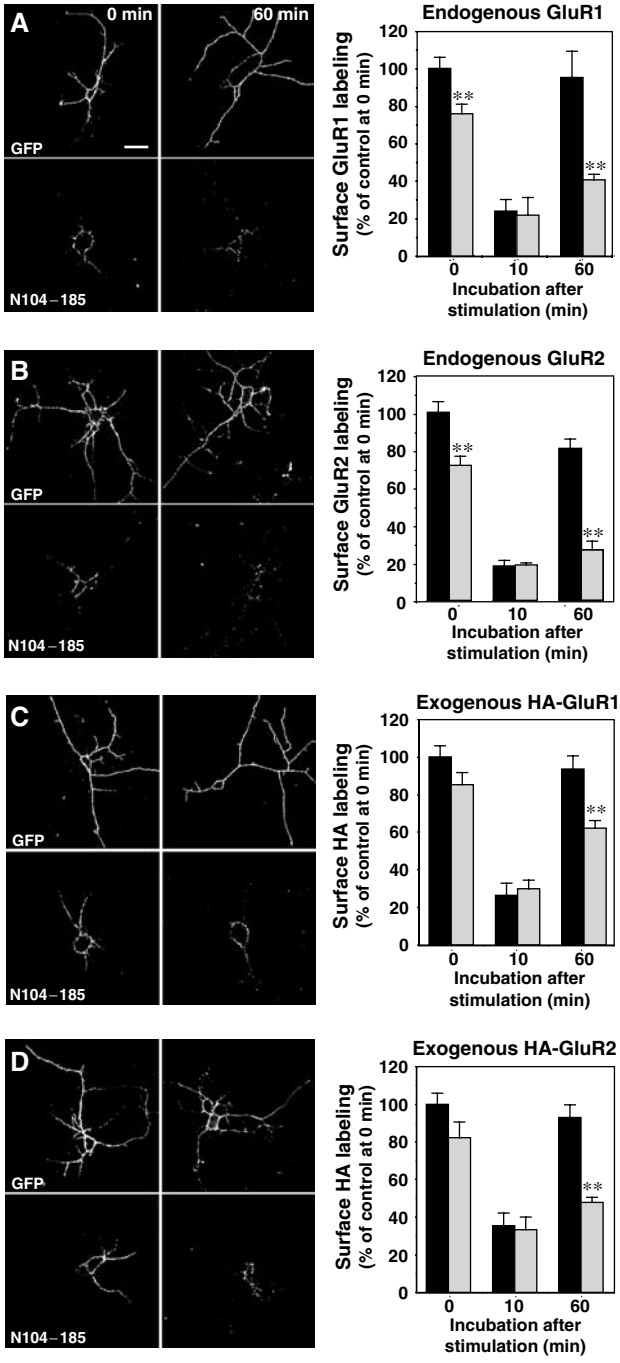

Figure 1 Expression of the entire cytosolic domain of NEEP21 perturbs GluR1 and GluR2 cycling. (**A, B**) Hippocampal neurons at DIV8 were transfected with GFP (black bars) or GFP fused to aa104–185 of NEEP21 (gray bars). At DIV10, cells were preincubated with TTX for 1 h and fixed (0 min, images on the left row) or stimulated for 2 min with 50 μM NMDA and further incubated for a total of 10 or 60 min (images on the right row) before fixation. Then, surface GluR1 (A) or GluR2 (B) was revealed by immunolabeling without permeabilization using extracellularly binding antibodies. Fluorescence was quantified on confocal images. 100% corresponds to integrated fluorescence intensity of the GFP-transfected cells at 0 min. (**C, D**) As in panels A and B, except that neurons were cotransfected with HA-GluR1 (C) or HA-GluR2 (D), and an anti-HA antibody was used for surface labeling. Scale bar, 10 μm; $^{**}P<0.01$, differences between black bar and gray bar at a given time point.

recycling of both GluR1 (Figure 1C) and GluR2 (Figure 1D) was retarded by GFP-N104–185. These results show that the cytosolic domain of NEEP21 interferes with the recycling of the AMPAR subunits GluR1 and GluR2, in agreement with our previous result using antisense suppression (Steiner *et al*, 2002).

In order to elucidate the mechanism involving NEEP21 in AMPAR cycling, we sought to identify protein complexes containing NEEP21 by immunoprecipitation from rat brain membrane extracts. Anti-NEEP21 immunopellets contained the PDZ protein GRIP1 (Figure 2A), a scaffolding molecule involved in trafficking of membrane receptors including GluR2. We also identified GRIP1 in anti-syntaxin 13 immunoprecipitations, but not in control precipitations with nonspecific IgG. We then asked whether NEEP21 also associates with AMPAR. Indeed, we observed faint, but clear GluR2 immunoreactivity (Figure 2B). GluR2 was shown to bind to the general trafficking proteins NSF/αSNAP (Song *et al*, 1998; Noel *et al*, 1999). We did not detect αSNAP in NEEP21 immunoprecipitates (Figure 2B), suggesting different interactions. Also, the PDZ proteins SAP97, a protein involved in GluR1 trafficking, and PSD-95 were not detected (Figure 2B, arrow indicates full-length SAP97 band). As further controls, we analyzed for co-precipitation of the SNARE proteins syntaxin 1 and VAMP2, and the integral synaptic vesicle protein synaptophysin, which were all negative (Figure 2B). Co-precipitation of GRIP1, GluR2 and syntaxin 13 with NEEP21 could also be confirmed using CHAPS instead of Triton X-100 to solubilize membranes (data not shown).

In order to further define NEEP21/GRIP1/AMPAR interactions, we investigated their relative size distribution by size-exclusion chromatography (Figure 2C), which separates protein complexes according to their globular sizes. NEEP21 eluted from the column at a peak around 250 kDa and at another clearly separated high-molecular-weight peak that we estimate to be about 650–900 kDa (herein called 800 kDa peak; note that fractions 1–3 belong to the column void volume). Syntaxin 13, SAP97, GluR2 and GluR1 eluted over wide size ranges, with maxima at about 300 kDa for syntaxin 13, about 700 kDa for SAP97 and around 600 kDa for both AMPAR subunits. GRIP1 eluted with two recognizable peaks at around 400 kDa, containing the majority of GRIP1, and a

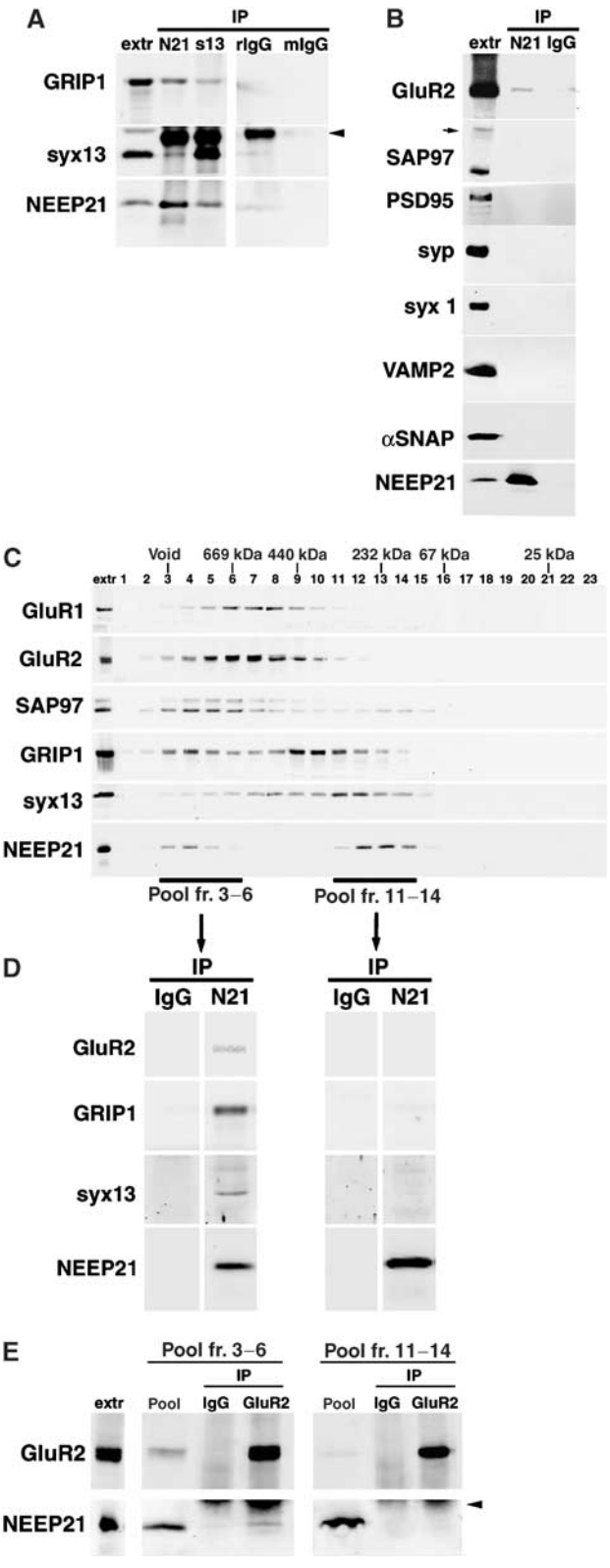

Figure 2 NEEP21, GRIP1, GluR2 and syntaxin 13 are present in 600–900 kDa complexes. (**A**) Antibodies crosslinked to beads (N21, anti-NEEP21; s13, anti-syntaxin 13; rIgG, rabbit IgG; mIgG, mouse IgG) were incubated with rat brain membrane extract (1.6 mg) and immunoprecipitated proteins (IP) analyzed by Western blotting for the indicated proteins (syx13, syntaxin 13; extr, crude input extracts corresponding to 1/20 of immune pellets). The arrowhead indicates crossreacting antibody heavy chain. (**B**) As in panel A. Anti-NEEP21 antibodies co-precipitate GluR2, but not SAP97, PSD95, synaptophysin (syp), syntaxin 1 (syx1), VAMP2 or αSNAP. SAP97 appears at 140 kDa (arrow) and an additional, presumably degradation product at about 90 kDa in extract lane, as described previously (Muller *et al*, 1995). (**C**) Rat brain membrane extract (6 mg) was separated on a Superdex 200 size-exclusion chromatography column and fractions were analyzed by Western blotting for the indicated proteins. The column was calibrated in parallel runs using the following as standards: Blue Dextran, void volume; thyroglobulin, 669 kDa; ferritin, 440 kDa; catalase, 232 kDa; albumin, 67 kDa; chymotrypsin, 25 kDa. NEEP21 elutes in two distinct peaks around 800 and 250 kDa. (**D**) Fractions 3–6 or 11–14, containing NEEP21 around 800 or 250 kDa, respectively, were pooled from five column runs and loaded sequentially on a nonspecific rabbit IgG (rIgG) column and then on a specific anti-NEEP21 immunoaffinity column. Eluted proteins were analyzed. Note that GluR2, GRIP1 and syntaxin 13 co-precipitate with NEEP21 from 800 kDa fractions, but not from 250 kDa fractions. (**E**) As in panel D, but using non-crosslinked mouse IgG and then mouse anti-GluR2 for immunoprecipitation. Co-precipitation of NEEP21 was detected only in 800 kDa fractions.

second peak at around 800 kDa. Interestingly, the latter showed clear overlap with the 800 kDa peak of NEEP21.

Given these partially overlapping distribution profiles, we wondered whether GluR2 and GRIP1 associated with NEEP21 either in the 800 kDa or the 250 kDa peaks. Therefore, we pooled the NEEP21-positive fractions 3–6 (around 800 kDa) and 11–14 (around 250 kDa), preabsorbed them to nonspecific IgG beads (Figure 2D, IgG) and immunopurified NEEP21 from both pools on specific anti-NEEP21 antibody beads (Figure 2D, N21). We found that GRIP1, GluR2 and syntaxin 13 were selectively co-immunopurified from fractions 3–6, but not from fractions 11–14 (Figure 2D). No signals for GluR1 and SAP97 could be detected (data not shown).

In reciprocal precipitations, we subjected the NEEP21-positive fractions 3–6 (250 kDa pool) and 11–14 (800 kDa pool) to anti-GluR2 immunoprecipitations (Figure 2E). In line with the result in Figure 2D, we detected a small, but specific amount of co-precipitated NEEP21 only from the 800 kDa pool. These results clearly suggest that large NEEP21 complexes include interactions between NEEP21, GRIP1, syntaxin 13 and GluR2-containing AMPAR.

A NEEP21 fragment of 35 aa interacts directly with GRIP1

In a next step, we wanted to elucidate which domains of NEEP21 and GRIP1 are involved in this interaction. We carried out pull-down experiments using rat brain membrane extracts and immobilized fusion proteins between glutathione-*S*-transferase (GST) and different fragments of the carboxy-terminal, cytosolic part of NEEP21 (Steiner *et al*, 2002). The complete cytosolic domain (aa104–185) was able to pull down GRIP1 (Figure 3B). Wherever neither aa104–134 nor aa167–185 recruited significant amounts of GRIP1 signals, the fragment aa129–164 resulted in a strong GRIP1 signal. The same fragments could also recruit GluR2/3, while no GluR1 signals were detected (Figure 3B). Also, the unrelated membrane protein L1 was not detected (data not shown), verifying the specificity of the observed interactions. These results thus provided additional evidence for interactions between NEEP21, GRIP1 and GluR2/3, and pointed to a critical 35 aa stretch containing the binding region in NEEP21. To analyze whether there is a direct binding between NEEP21 and GRIP1, we used a purified recombinant fragment of GRIP1. There was a clear binding of this soluble GRIP1-aa810–1112 to GST-N104–185 and, although weaker, to GST-N129–164, but not to control GST beads (Figure 3C).

We then investigated further the binding between NEEP21, GRIP1 and GluR2 (as GST fusion proteins) using atomic force microscopy (AFM). This technique allows a direct and quantitative analysis of an interaction between a protein on the tip of the AFM cantilever and another protein on the mica surface (Florin *et al*, 1994; Yersin *et al*, 2003). In a first experiment, we measured the established interaction between GluR2 and GRIP1. The carboxy-terminal cytosolic domain of GluR2 (GluR2ct) was fixed to the AFM tip, and a GRIP1 fragment aa342–809 to the mica surface. After 1200 contact–retraction cycles, we observed interaction events with an average relative binding force of 109 ± 10 pN and a binding probability (defined as the ratio of number of binding events divided by number of contact–retraction cycles) that was clearly higher than the negative control between GluR2ct and nonspecific GST (Figure 3D). This confirms the previously shown interaction between GluR2 and PDZ domains 4 and 5 (Dong *et al*, 1997) contained in GRIP1-aa342–809. When the same GRIP1 fragment was tested against the cytosolic domain of NEEP21 (NEEP21ct), we could not observe a significant interaction (Figure 3E). In contrast, NEEP21ct bound to the carboxy-terminal GRIP1-aa810–1112 (Figure 3F) with an average relative interaction force of 111 ± 8 pN. NEEP21ct did not interact with GluR2ct (Figure 3G), suggesting no direct binding. We further confirmed the interaction between NEEP21ct and a long fragment GRIP1-aa342–1112 by on-line AFM measurements. While injection of soluble GRIP1-aa342–809 into the AFM chamber had no effect (Figure 3H), injection of GRIP1-aa810–1112 caused a significant reduction of the continuously recorded binding events (Figure 3I), presumably by competing with the GRIP1 fragment on the mica surface.

We then tested whether full-length GRIP1 promotes binding between NEEP21 and GluR2. To this end, HEK293T fibroblast cells were cotransfected with tagged NEEP21, GluR2 and either GFP (as control) or GRIP1, followed by NEEP21 immunoprecipitation (Figure 3J). We detected a weak, but clear co-precipitation of GluR2 in the absence of GRIP1, which might be linked to endogenous GRIP1 in fibroblast cell lines, as detected by Western blot (not shown). The presence of GRIP1 induced a modest increase in GluR2 co-precipitation (1.52-fold after normalization on precipitated NEEP21).

The above pull-down assays showed that fragment aa129–164 of NEEP21 contains a GRIP1-binding site. To analyze if this fragment could interfere in cells with the binding between NEEP21 and GRIP1, HEK293T cells were cotransfected with NEEP21, GRIP1 and either GFP or GFP tagged with aa129–164 of NEEP21 (GFP-N129–164). Following NEEP21 immunoprecipitation, the presence of this fragment caused a marked decrease in the amount of co-precipitated GRIP1 (Figure 3K).

Together, these data show that NEEP21 interacts directly with GRIP1. Moreover, the NEEP21-binding domain on GRIP1 is in the carboxy-terminal 303 aa, while the GRIP1-binding site on NEEP21 is located on fragment aa129–164.

NEEP21–GRIP1 interaction regulates synaptic GluR2-AMPAR insertion

In order to assess the effect of NEEP21–GRIP1 interaction on receptor trafficking in neurons, we tested the effect of the GRIP1-binding domain of NEEP21 (aa129–164) on GluR1 and GluR2 cycling described in Figure 1. We noticed a reduced dendrite length upon GFP-N129–164 transfection, but overall transport of other dendritic and synaptic proteins appeared to be normal (Supplementary Figure 1). Hippocampal neurons, transfected with either GFP or GFP-N129–164, were preincubated with TTX and stimulated with NMDA, followed by surface labeling of GluR1 and GluR2 (Steiner *et al*, 2002). Before stimulation, GFP-N129–164-expressing neurons had significantly lower GluR2 levels at the surface (Figure 4B, gray bars) than GFP-expressing neurons (Figure 4B, black bars). At 10 min after stimulation, there was efficient internalization of GluR2 in both cell batches. In contrast, while in GFP-expressing neurons, GluR2 reappeared at the surface to almost initial values at 60 min, surface GluR2 levels were substantially decreased in GFP-N129–164-expressing neurons (Figure 4B, 60 min). Despite the strong effect on GluR2

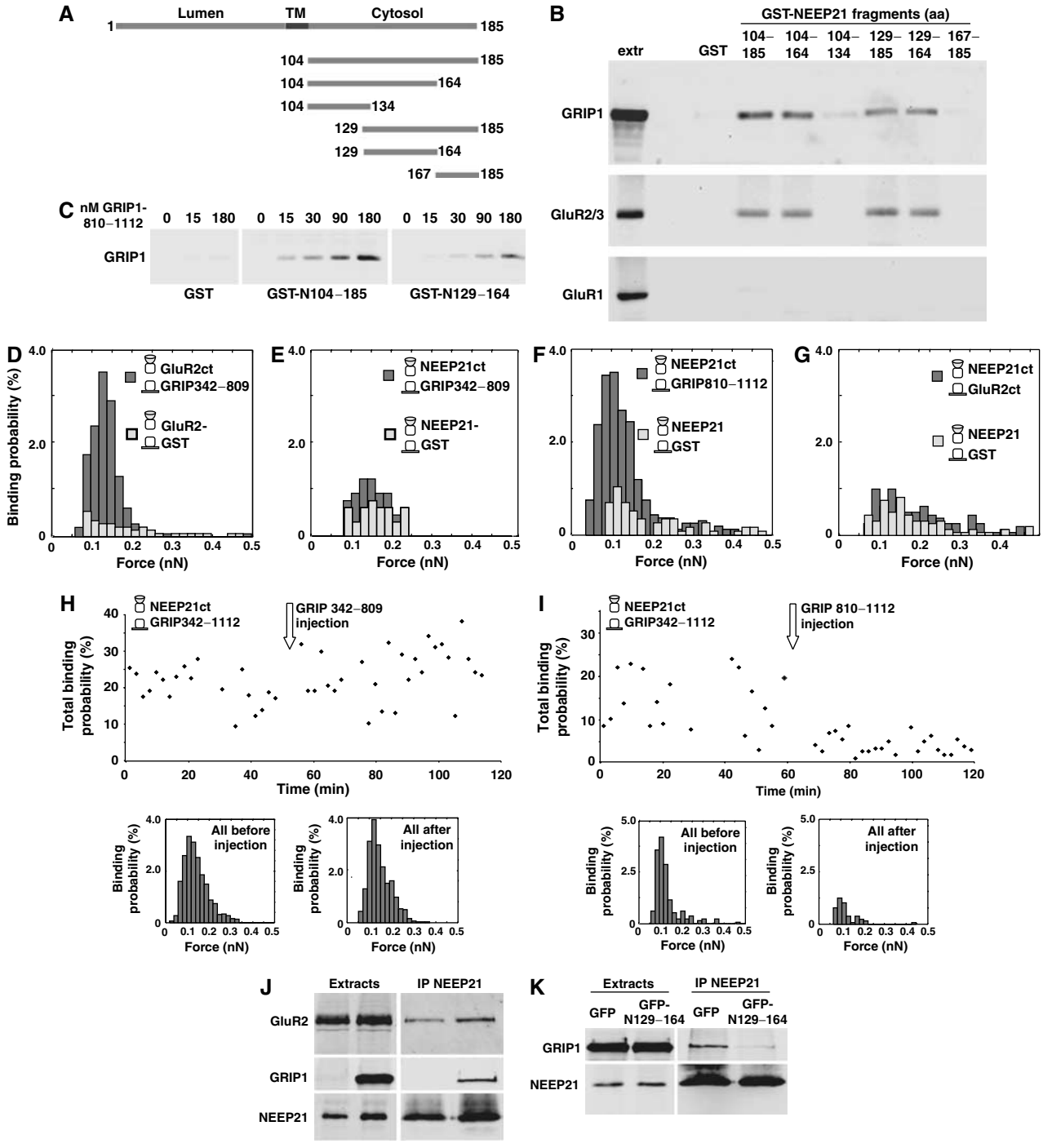

Figure 3 A fragment aa129–164 of NEEP21 interacts with GRIP1. (**A**) Scheme of NEEP21 deletion constructs expressed as GST fusion proteins. TM, transmembrane region. (**B**) Immobilized GST fusion proteins were incubated with rat brain membrane extract and bound proteins analyzed on Western blot. (**C**) Binding assay between different amounts of purified recombinant GRIP1-aa810–1112 and immobilized GST, GST-N104–185 or GST-N129–164. GRIP1 binds directly to NEEP21. (**D**) Analysis by AFM of interactions between GRIP1 and GluR2 (all as GST fusion proteins). The carboxy-terminal 50 aa of GluR2 (GluR2ct) was crosslinked to the AFM tip, and either GST alone (gray bars, control) or GRIP1-aa342–809 (black bars) was crosslinked to the mica surface. After 1200 cycles, a binding probability of 23.4% (relative peak interaction force 109 ± 10 pN) was detected with GRIP1-aa342–809, which is significantly higher than the background probability with GST (4.4%). (**E**) As in panel D, but with the cytosolic domain of NEEP21 (NEEP21ct) on the tip. No significant binding was observed with this central GRIP1 fragment. (**F**) As in panel E, but with either GST or GRIP1-aa810–1112 on the mica. Binding probability is significantly higher than control levels (21.4%; relative peak interaction force 111 ± 8 pN), confirming direct interaction between NEEP21 and GRIP1. (**G**) As in panel E, but with either GST or GluR2ct on the mica. No significant binding was detected. (**H, I**) On-line observations of binding events between aa104–185 of NEEP21 (on AFM tip) and GRIP1-aa342–1112 (on mica), before and after injection (arrow) of soluble GRIP1-aa342–809 (H) or GRIP1-aa810–1112 (I). Only in the latter case, a significant decrease in binding probability ($P < 0.01$) was observed, suggesting competition by fragment aa810–1112 for binding between NEEP21 and GRIP1-aa342–1112. The histograms show all events before (left) or after (right) injection. (**J**) HEK293T fibroblast cells were cotransfected with NEEP21-EE, HA-GluR2 and either GFP or myc-GRIP1, as visible in the extract lanes, followed by anti-EE immunoprecipitation. There is a detectable co-precipitation of GluR2, which is enhanced (1.5-fold) by the expression of exogenous GRIP1. (**K**) HEK293T fibroblast cells were cotransfected with NEEP21-EE, myc-GRIP1 and either GFP or GFP-N129–164, followed by anti-EE immunoprecipitation. GFP-N129–164 reduces NEEP21–GRIP1 co-precipitation.

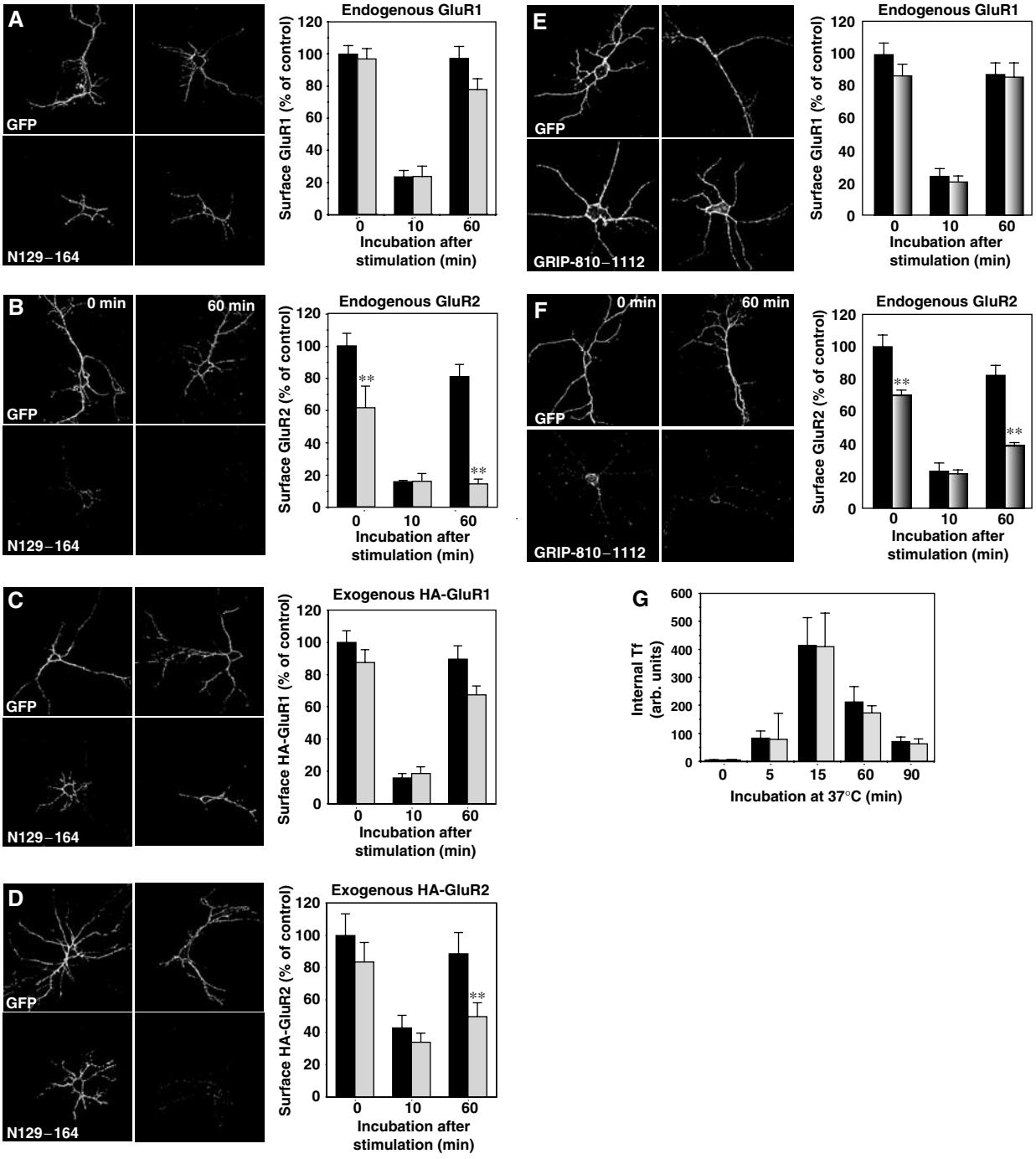

Figure 4 Expression of aa129–164 of NEEP21 and of aa810–1112 of GRIP1 perturb GluR2 cycling. (**A–D**) Hippocampal neurons were transfected, stimulated and labeled for surface GluR1 or GluR2 as in Figure 1, except that GFP (black bars), or GFP-N129–164 (gray bars) instead of the whole cytosolic domain, was used. (**E, F**) Surface labelings as in panels A and B, except that neurons were transfected with either GFP (black bars) or GFP fused to the carboxy-terminal aa810–1112 of GRIP1 (shaded bars). (**G**) Rhodamine-conjugated Tf was prebound on ice to hippocampal neurons cotransfected with human TfR and either GFP (black bars) or GFP-N129–164 (gray bars). Internalization and recycling of Tf was then allowed at 37°C. Surface Tf was removed by acid wash on ice before fixation. Internal Tf labeling on confocal images was quantified. GFP-N129–164 does not alter Tf recycling.

recycling, GFP-N129–164 caused only a slight, statistically not significant inhibition of GluR1 recycling (Figure 4A). This distinguishes this limited fragment from the whole cytosolic domain of NEEP21 presented in Figure 1 that affected both GluR1 and GluR2.

When analyzing homomeric HA-tagged GluR1 or GluR2, we observed again a clear inhibition on the surface reappearance of HA-GluR2 (Figure 4D), but not of HA-GluR1 (Figure 4C), by aa129–164. We did not find a difference in surface HA-GluR2 before stimulation, probably due to its overexpression. The effect of GFP-N129–164 on endogenous and exogenous GluR2, but not on GluR1, indicates that this fragment acts via GluR2 on the cycling of AMPAR that are presumably mainly GluR2/3-AMPAR.

Since aa129–164 interacted with the carboxy-terminal GRIP1 fragment aa810–1112 (see Figure 3C and F), we

wondered whether this GRIP1 fragment affects AMPAR cycling in a similar manner. Indeed, while internalization and recycling of GluR1 were not affected (Figure 4E), recycling of GluR2 was strongly retarded (Figure 4F), as observed above with aa129–164 of NEEP21. This result indicates that the carboxy terminus of GRIP1 is involved in AMPAR recycling.

In order to verify that GFP-N129–164 does not cause a general perturbation of the endosomal recycling pathway, we also analyzed the cycling of the ubiquitous TfR and its ligand Tf. Hippocampal neurons were transfected with the human TfR and either GFP or GFP-N129–164, and we measured the appearance and disappearance of fluorescent Tf in internal compartments, a phenomenon that reflects internalization and recycling (Steiner *et al*, 2002). GFP-N129–164 did not alter the Tf time course (Figure 4G), excluding a general effect of this small NEEP21 fragment on the endosomal recycling pathway. Also, it did not affect regulated secretion in a growth hormone release assay in PC12 cells (data not shown).

It has been shown that GluR2-lacking AMPAR exhibit particular electrophysiological features, such as inward rectification of excitatory post synaptic current (EPSC) current/voltage relationships (Hollmann *et al*, 1991) and Joro spider toxin (JST) sensitivity (Blaschke *et al*, 1993). Since aa129–164 specifically interfered with surface localization of GluR2 in dissociated hippocampal neurons, we tested its effect on AMPAR-mediated synaptic currents by whole-cell patch clamp recordings in CA1 hippocampal slice culture. We infused a peptide corresponding to aa129–164 (N129–164) through the patch pipette, and recorded evoked AMPAR-mediated synaptic activity at different holding potentials going from -80 to $+40$ mV, before and 30 min after peptide infusion (Figure 5A and B). While immediately after whole-cell access the EPSC current/voltage relationship was linear, it exhibited clear inward rectification at depolarized potentials after peptide infusion (Figure 5A and B; $n=16$). The rectification index, calculated by dividing the EPSC current amplitude at $+40$ mV by the one at -60 mV, was 0.77 ± 0.4 before and 0.31 ± 0.06 after peptide infusion (Figure 5A and C; $n=12$; $P<0.01$). This was further confirmed by JST (500 nM), a drug known to specifically block GluR2-lacking AMPAR (Blaschke *et al*, 1993). In control cells, bath application of JST did not affect the amplitude of evoked EPSCs, consistent with GluR2-containing AMPAR being expressed at synapses (data not shown). However, after 35 min of peptide infusion, application of JST reduced the amplitude of evoked EPSC at -80 mV by about 42% (Figure 5D; $n=5$; $P<0.05$). Control neurons, perfused with buffer alone, exhibited neither inward rectification nor JST sensitivity. In addition, infusion of N129–164 resulted in a run-down of synaptic transmission ($18\pm4\%$; $n=6$; $P<0.01$) similar to that observed with an NSF-interacting peptide (pep2m; $28\pm4\%$; $n=6$; $P<0.05$), suggesting an impairment of constitutive AMPAR recycling (Figure 5E and Supplementary Figure 2). These results strongly indicate that peptide N129–164 impairs surface expression of GluR2-containing AMPAR at synapses.

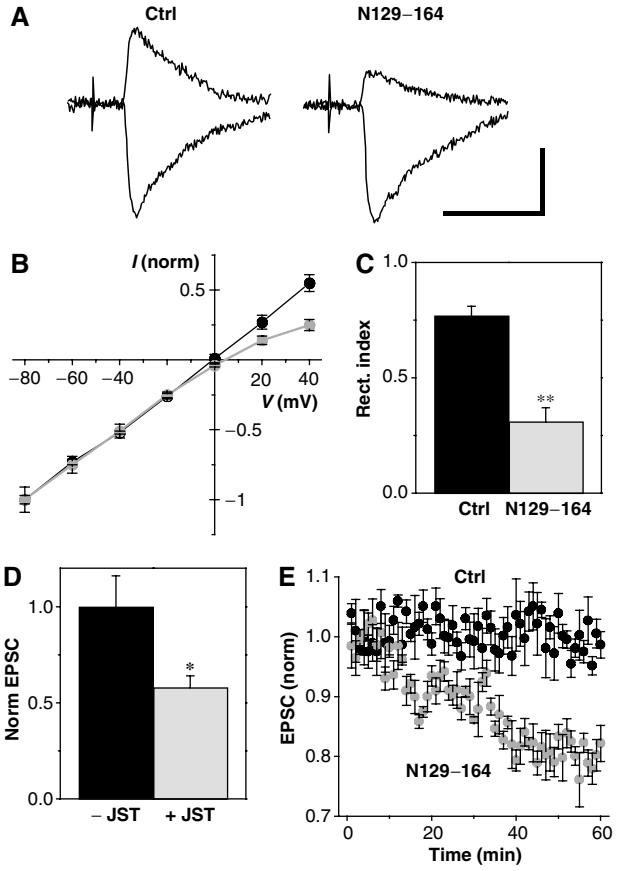

Figure 5 Infusion of a peptide N129–164 induces rectification in CA1 pyramidal neurons. (**A**) Mean evoked AMPAR-mediated EPSC traces taken at $+40$ mV and at -60 mV just after accessing whole-cell configuration (left) or 40 min after N129–164 infusion (right). Bars: 40 pA; 25 ms. (**B**) The linear *I*/*V* relationship of synaptic AMPA EPSCs observed in the absence of N129–164 (black circles) became inwardly rectifying after infusion of the peptide (gray circles; $n=16$). (**C**) N129–164 infusion modifies the rectification index ($+40/-60$ mV; $n=12$; $^{**}P<0.01$). (**D**) JST (500 nM) blocked the evoked EPSC after 30 min of N129–164 infusion ($n=5$; $^{*}P<0.05$). (**E**) Infusion of peptide N129–164 decreases AMPAR-mediated synaptic responses. Time course of changes in EPSC amplitude measured in control cells (black circles) and in adjacent cells infused with peptide N129–164 (gray circles; $n=6$). Data are means$\pm$s.e.m.

NEEP21 promotes sorting of GluR2 to the recycling pathway

It has previously been shown that brief application of NMDA to hippocampal neuron cultures in combination with TTX preincubation induces rapid AMPAR internalization and recycling (Ehlers, 2000; Lee *et al*, 2004), while stimulation with NMDA alone causes internalization and sorting to the degradation pathway (Lee *et al*, 2004). In order to analyze whether the NEEP21–GRIP1–GluR2 binding is modulated under these conditions of differential AMPAR sorting, we carried out anti-NEEP21 immunoprecipitations from control cells, NMDA/TTX-stimulated cells or NMDA-stimulated cells. From control neurons, we co-precipitated GRIP1 with NEEP21 (Figure 6A and B). This signal is significantly enhanced in cells that had been preincubated with TTX and briefly stimulated with NMDA (2.3-fold; recycling condition), while stimulation with NMDA alone causes a significant decrease in GRIP1 co-precipitation (0.48-fold; degradation condition). When blots from these immunoprecipitations were probed for GluR2, we detected the same profile (Figure 6C). This strongly suggests that NEEP21–GRIP1–GluR2 interactions are increased in living neurons under

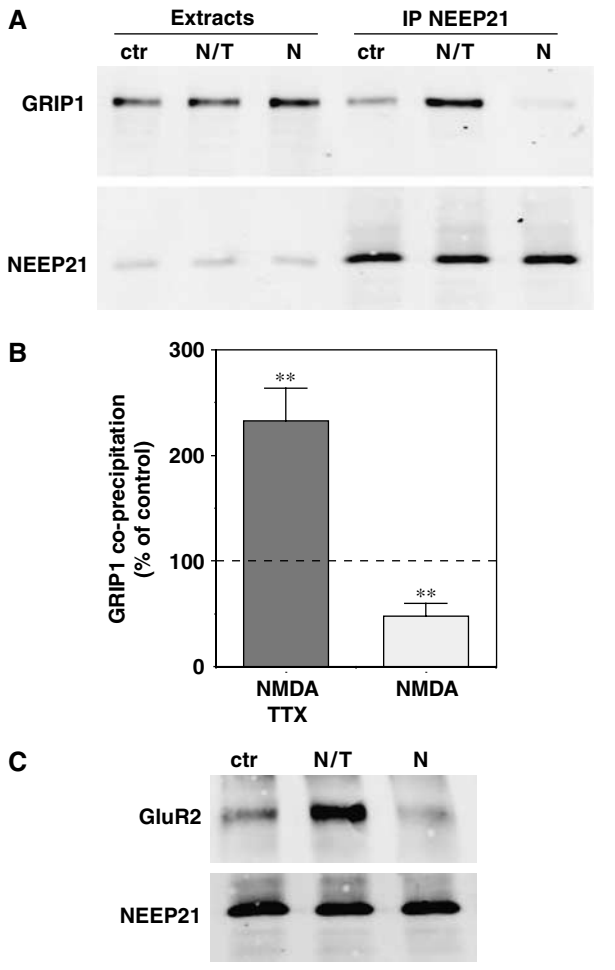

Figure 6 NEEP21–GRIP1–GluR2 interactions are regulated by NMDA stimulation. (**A**) Hippocampal neurons were either left unstimulated (ctr) or preincubated for 1 h with TTX (2 μM) and then stimulated with 50 μM NMDA for 2 min (N/T), or only stimulated with 50 μM NMDA for 2 min (N). N/T and N were further incubated for 2 min without NMDA. Neurons were lysed and subjected to anti-NEEP21 immunoprecipitation, followed by blotting for NEEP21 and GRIP1. Crude extracts and immunopellets (IP NEEP21) were loaded. (**B**) Pixel intensities on images from four experiments as in (A) were quantified. The graph shows the relative amount of co-precipitated GRIP1 normalized to precipitated NEEP21. 100% corresponds to unstimulated cells. Co-precipitated GRIP1 is significantly increased upon NMDA/TTX stimulation and decreased upon NMDA stimulation ($P<0.02$). (**C**) Blot as in (A) was reprobed for the co-precipitation of GluR2.

conditions of receptor recycling, and decreased when receptors are sorted for degradation.

The inhibition of GluR2 surface expression by GFP-N129–164 suggested that it is blocked in an internal compartment. We therefore analyzed colocalization of internalized HA-GluR2 with the early endosomal marker EEA1 (Figure 7A and B) or the lysosomal marker LAMP1 (Figure 7C and D) in NMDA/TTX-stimulated neurons that had been transfected with either GFP or GFP-N129–164. In control GFP-transfected cells, we found a transient appearance of GluR2 in early endosomes (37.3% at 10 min and 16.6% at 30 min) in line with previous data (Ehlers, 2000; Lee *et al*, 2004), and a low colocalization with LAMP1 (12.9% at 10 and 30 min), verifying a low degree of sorting to degradation. In contrast, GFP-N129–164 led to a strong accumulation of HA-GluR2 in early endosomes at 30 min (71.8%), a time point when cycling receptors have normally been sorted to downstream pathways (Ehlers, 2000; Lee *et al*, 2004). Moreover, there is an aberrant sorting of HA-GluR2 to lysosomes at 30 min (27.5%). As negative control, we analyzed colocalization between internal GluR2 and the synaptic vesicle protein VAMP2, which was equally low under all conditions (Figure 7E and F). Total expression levels of HA-GluR2 (surface plus internal) were equal in neurons expressing GFP (100%) or GFP-N129–164 (97.9%). Together, these results are in line with an essential function of NEEP21 protein interactions in the exit of internalized receptors from early endosomes and traffic toward the recycling pathway.

Discussion

Synaptic transmission and plasticity rely on variations in the number of AMPA-type glutamate receptors inserted into the postsynaptic plasma membrane. These receptors are recruited from or internalized into endosomes, but the molecular mechanisms governing intracellular receptor transport through these organelles are not well understood. We show here that the endosomal protein NEEP21 associates with the PDZ scaffolding molecule GRIP1 and the AMPAR subunit GluR2. Interfering with this interaction by expression of the GRIP1-binding site of NEEP21 specifically affects GluR2 surface expression, causes GluR2 accumulation in early endosomes and results in alterations of the properties of evoked synaptic currents.

We have previously found that suppression of NEEP21 by an antisense construct causes retardation of recycling not only of GluR2 but also of GluR1 in hippocampal neurons, and even of the ubiquitous TfR in PC12 cells (Steiner *et al*, 2002). This is confirmed here by the effect of overexpression of the cytosolic domain of NEEP21 that affected cycling of both GluR1 and GluR2. In contrast, expression of the small fragment aa129–164 that interacts with GRIP1 does not affect GluR1 or TfR. This suggests that interactions apart from that with GRIP1 occur on NEEP21 and are responsible for regulation of a larger range of receptors. It is not clear why we did not detect significant signals for GluR1 associated with NEEP21. A likely explanation is that, in contrast to GluR2 receptors, the GluR1-containing receptors do not cycle constitutively (Shi *et al*, 2001). Therefore, only extremely small, undetectable amounts might be present in NEEP21-containing complexes.

Through size-exclusion chromatography, we found that NEEP21 exists in two distinct protein complexes of around 250 and 800 kDa, with GRIP1 and GluR2 associated with NEEP21 only in the latter one. As NEEP21 is also involved in the cycling of receptors other than AMPAR (Steiner *et al*, 2002; Debaigt *et al*, 2004), NEEP21 molecules at 250 and 800 kDa are most probably engaged in further interactions, in addition to the ones described here. Moreover, the majority of GluR2 is presumably in AMPAR at the plasma membrane and in other endosomal compartments.

Pull-down assays and AFM showed that GRIP1-aa342–809, containing the GluR2-interacting PDZ domains 4 and 5 (Dong *et al*, 1997), bound to GluR2, while the carboxy-terminal GRIP1-aa810–1112 bound to NEEP21. This latter GRIP fragment contains PDZ domain 7, which has previously been

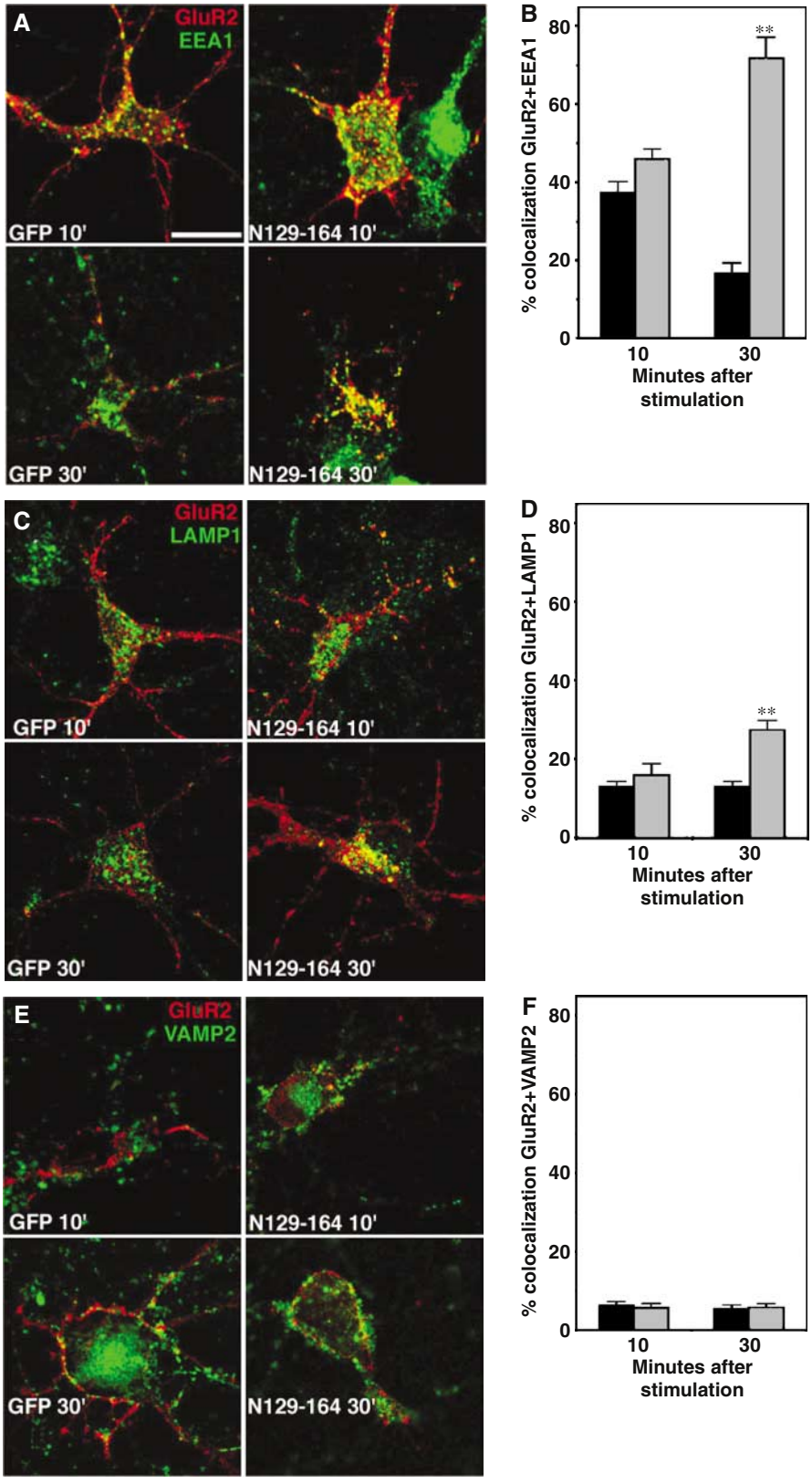

Figure 7 Expression of aa129–164 causes accumulation of internalized GluR2 in early endosomes and lysosomes. Hippocampal neurons, transfected with HA-GluR2 and either GFP (black bars in **B, D, F**) or GFP-N129–164 (gray bars in B, D, F), were incubated with extracellularly binding anti-HA antibody (red pseudocolor in **A, C, E**), stimulated with NMDA/TTX as in Figure 4, and further incubated for 10 or 30 min. Then cells were acid washed to remove extracellular labeling, fixed and colabeled for the early endosome marker EEA1 (green in A), the lysosomal marker LAMP1 (green in C) or the synaptic vesicle protein VAMP2 (green in E). Secondary antibodies were conjugated to Cy5 (green) or Cy3 (red). In each case, colocalization over cell bodies of at least 30 cells was quantified. Error bars, s.e.m. $^{**}P<0.01$, differences between GFP and GFP-N129–164. Scale bar, 20 μm.

found to be involved in nonconventional PDZ interactions (Feng *et al*, 2002). It is however unclear whether PDZ 7 is involved in NEEP21 binding. We used AFM because it directly measures interaction forces between single proteins. Since this force depends on the loading rate, all our measurements were accomplished by keeping this parameter constant. Multiple ruptures of protein–protein pairs can be excluded, since they would result in the presence of additional peaks at multiple interaction forces, which did not occur in the presented study.

To investigate the functional implication of this NEEP21–GRIP1 interaction in AMPAR trafficking and synaptic transmission, we used the dominant-negative NEEP21 fragment aa129–164 that interfered with this interaction. Expression of aa129–164 in hippocampal neurons markedly reduced surface expression of GluR2, but not of GluR1. Therefore, it is likely that the limited fragment aa129–164 affects specifically trafficking of the GluR2 subunit in AMPAR. These might include some GluR1/2 receptors passing through the recycling pathway, but the main effect is likely to concern fast-cycling GluR2/3 receptors. This is consistent with our recent study showing that interference with NEEP21 expression results in a reduction of spontaneous miniature synaptic response amplitude, a reduced AMPA/NMDA ratio and a lack of enhancement of evoked synaptic responses following blockade of endocytosis (Alberi *et al*, 2005). All these results thus clearly point to a role of NEEP21 in constitutive cycling. Interestingly, infusion of the peptide N129–164 resulted in increased rectification of AMPAR-mediated responses and increased sensitivity to JST, signatures that can be attributed to a selective decrease in synaptic GluR2-containing AMPAR. This differs from the GluR2-NSF-interacting peptide pep2m, which causes run-down of the responses, but no significant rectification in hippocampal slices (Terashima *et al*, 2004; Supplementary Figure 2). This indicates therefore that the effects observed upon interference with NEEP21 are not simply a nonspecific consequence of removing AMPAR from the synapse. They rather reflect a direct contribution of NEEP21–GRIP1 interaction to the regulation of the subunit composition of AMPAR, possibly at the level of receptor sorting. Indeed, aa129–164 provoked an accumulation of GluR2 in early endosomes and an increased targeting to lysosomes, in agreement with our previous localization of NEEP21 on early sorting endosomes.

In dissociated cultures, NMDA stimulation in combination with TTX preincubation (which blocks sodium channels and thereby eliminates spontaneous activity) enhances internalization and recycling of AMPAR (Ehlers, 2000; Lee *et al*, 2004), as does agonist stimulation with AMPA (Lee *et al*, 2004). Curiously, stimulation with NMDA in the absence of TTX induces sorting to the degradation pathway (Lee *et al*, 2004). This has been suggested to be linked to synaptic scaling, an adaptation of the neuron to the overall activity status in the network (Turrigiano and Nelson, 2004). Interestingly, we found that co-precipitation of GRIP1 and GluR2 with NEEP21 is enhanced under conditions of AMPAR recycling, while it is decreased under conditions of AMPAR degradation. This is a strong indication that the protein interactions discovered here are directly linked to the regulation of intracellular AMPAR sorting, and might allow the cell to adapt to long-term changes in activity levels. The enhanced interaction by NMDA/TTX occurred quickly, within 4 min after stimulation, and could presumably coincide with the arrival of endocytosed receptors in early endosomes where the stimulus-dependent sorting into the recycling or degradative pathways takes place (Ehlers, 2000; Lee *et al*, 2004). This is in line with our previous study on the subcellular localization of NEEP21 on a Rab4 domain of early endosomes. Since the fragment aa129–164 behaves in a dominant-negative manner in GluR2 surface reappearance and AMPAR properties, and blocks cycling receptors in early endosomes, we propose a model (Figure 8) in which the interaction between NEEP21 and GRIP1 would promote sorting of internalized receptors through endosomes and toward recycling compartments, before being inserted into the plasma membrane. This hypothesis is supported by the finding that anti-syntaxin 13 immunoprecipitates contained not only NEEP21 but also GRIP1 and that syntaxin 13 is present in the 800 kDa NEEP21-positive complex. Syntaxin 13 is a membrane trafficking SNARE mainly detected on recycling endosomes (Prekeris *et al*, 1998; Hirling *et al*, 2000) and also on early endosomes (McBride *et al*, 1999). Co-immunoprecipitation of GRIP1 with syntaxin 13 and of syntaxin 13 with NEEP21 suggests that at least some fraction of NEEP21–GRIP1 complexes becomes associated with components of the general recycling machinery during intracellular receptor trafficking. In a recently proposed modular organization of receptor sorting (Gage *et al*, 2005), NEEP21 could act as a link between the general membrane trafficking components and the sorting of a specific group of receptors. It will be important to investigate whether sorting signals like ubiquitination or other modifications can influence the observed

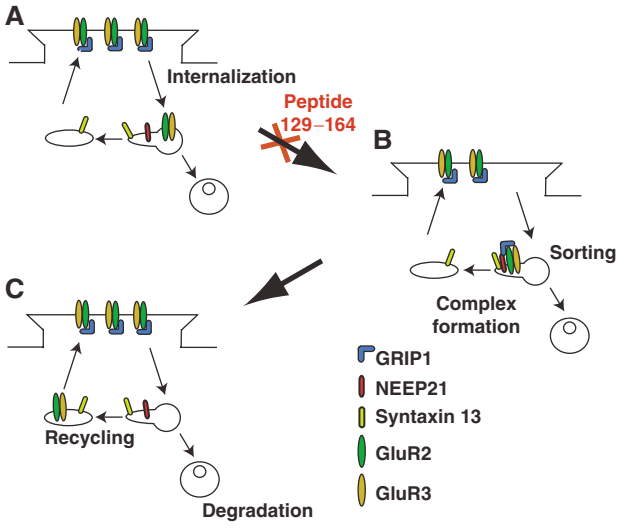

Figure 8 Model for a role of NEEP21 in GluR2 sorting. (**A**) NEEP21 is localized to early endosomes (Steiner *et al*, 2002), and syntaxin 13 to early and recycling endosomes (Prekeris *et al*, 1998; McBride *et al*, 1999). GluR2-containing AMPAR are at the postsynaptic density, and are internalized and appear on early endosomes. (**B**) According to this model, interactions between NEEP21, GRIP1, GluR2 and syntaxin 13 promote receptor sorting into the recycling pathway. Fusion events involving syntaxin 13 might occur during the transfer between the endosomal compartments. (**C**) Receptors can be recycled back to the cell surface from recycling endosomes. The dominant-negative fragment aa129–164 of NEEP21 might interfere with complex formation at the sorting step, causing impairment of GluR2 surface expression, its accumulation in early endosomes and aberrant sorting to degradation, and rectification of AMPAR currents.

interactions. In any case, the protein interactions discovered here might target GluR2 to tubular areas of early endosomes representing the exit domain toward recycling (Figure 8).

In conclusion, this study identified interactions between NEEP21, GRIP1, GluR2 and syntaxin 13 as a key regulatory mechanism that could control the intracellular fate of AMPAR and the endosomal sorting of the GluR2 subunit toward recycling and membrane targeting.

Materials and methods

Immunoprecipitation and pull-down experiments

Membrane pellets from rat brain (postnatal day 10) were prepared as described (Steiner *et al*, 2002) and lysed in buffer B (20 mM HEPES/KOH pH 7.4, 2 mM EDTA, 2 mM EGTA, 0.1 mM DTT, 0.1 M KCl, 1% Triton X-100; 5 ml per 1 g brain tissue). For immunoprecipitation and Western blotting (Steiner *et al*, 2002), antibodies crosslinked to protein A- or G-Sepharose (10 μl) were incubated with 1.6 mg of membrane extract for 4 h, washed with buffer B and eluted with 100 mM glycine, pH 2.5. For immunoprecipitation using non-crosslinking conditions, extracts were incubated for 2 h with 5 μl of anti-NEEP21 antibody, or 4 μl of monoclonal anti-GluR2 antibody, followed by addition of 10 μl of protein A- or protein G-Sepharose beads and further incubation for 1 h. Beads were washed and loaded onto SDS–PAGE for Western analysis. For GST pull-down assays, 1.8 mg of membrane extract was incubated for 1 h with GST fusion protein beads. After three washing steps, bound protein was analyzed by Western blots.

Interaction force measurement by AFM

AFM tips and substrates were prepared as described previously (Yersin *et al*, 2003). Briefly, recombinant GST fusion proteins (200–300 ng/μl) were covalently crosslinked by glutaraldehyde (0.5%) to the AFM tip (Digital Instruments, Santa Barbara, USA; nominal spring constant 0.06 N/m, calibrated by thermal noise analysis) and to a freshly cleaved mica sheet that had been functionalized by aminopropyltriethoxysilan (APTES). Experiments were performed at room temperature on a Nanoscope III® (Digital Instruments) with force volume mode operating in TBS buffer, at a constant retraction speed of 355 nm/s. Force curves were then analyzed off-line by a fuzzy logic algorithm (Yersin *et al*, 2003).

Size-exclusion chromatography

The membrane extract was prepared as described above, at a protein concentration around 24 mg/ml. A Superdex 200 size-exclusion chromatography column on an Äkta FPLC system (Amersham) was equilibrated in buffer B. The membrane extract (250 μl) was injected and fractions (500 μl) were collected at 0.5 ml/min. The column was calibrated under identical conditions using kits of proteins with known globular sizes (Amersham). Fractions 3–6 (150–350 kDa) or 11–14 (650–950 kDa) were pooled from five separations to immunopurify NEEP21 complexes from the 800 or 250 kDa fractions, respectively. These pools were incubated in a column with 80 μl of nonspecific rabbit IgG beads for 40 min, and then the flow-through was incubated overnight in a column with anti-NEEP21 antibody beads. Both columns were washed and eluted with 100 mM glycine pH 2.5. NEEP21 complexes were analyzed by Western blotting.

Cell culture and immunofluorescence

Rat hippocampal neuron cultures, neuron transfection, immunofluorescence and cycling of endogenous GluR1,2 and of HA-tagged GluR1,2 (Passafaro *et al*, 2001) were performed as described (Steiner *et al*, 2002). See also Supplementary data. We observed a reduced dendrite length in GFP-N129–164-transfected neurons (36%) compared to control neurons, which was partially, but significantly compensated by overexpression of HA-GluR2 (52%; $P = 0.01$). Double stainings between GluR2 and either PSD-95, NR1, MAP2 or synaptophysin suggested overall correct dendritic transport and synapse formation in GFP-N129–164-transfected neurons (Supplementary Figure 1).

For localization of internalized HA-GluR2, transfected neurons were incubated for 1 h at 37°C with TTX (2 μM) and for 10 min with TTX and anti-HA antibody to label surface HA-GluR2. Neurons were stimulated with 50 μM NMDA for 2 min, washed and further incubated for the indicated durations. Neurons were washed with PBS/30 mM glycine pH 2.5 to remove the remaining surface label, fixed and immunolabeled using antibodies against EEA1, LAMP1 or VAMP2. Colocalization using Metamorph software was quantified as described previously (Steiner *et al*, 2002) and detailed in Supplementary data. Colocalization is defined as the pixels that are positive for both internal GluR2 and EEA1, LAMP1 or VAMP2. The 100% in Figure 7 corresponds to the sum of pixels that are red or green, while colocalization corresponds to pixels that are red and green at a set threshold.

To analyze the modification of the NEEP21–GRIP1 interaction, neurons were either not treated, or stimulated for 2 min with 50 μM NMDA, or incubated for 1 h with TTX (2 μM) and then 50 μM NMDA was added. Washed neurons were further incubated for 2 min at 37°C, lysed in buffer B, cleared at 10 000 *g* for 10 min and supernatants incubated at 4°C for 4 h with 10 μl of anti-NEEP21-protein A beads.

HEK293T cells were cultured in DMEM/10% FCS, transfected using the calcium phosphate technique and lysed in buffer B for immunoprecipitation using anti-EE protein G beads.

Electrophysiology

Hippocampal organotypic slice cultures were prepared as described (Stoppini *et al*, 1991). Whole-cell recordings were performed on CA1 pyramidal cells of continuously superfused slices at DIV10. The bipolar stimulating electrode was placed in the stratum radiatum at $\geqslant$100 μm from the recorded cell soma. Evoked glutamatergic NBQX-sensitive AMPAR-mediated synaptic responses were induced at a frequency of 0.05–0.5 Hz throughout the experiment in the presence of $GABA_A$ and NMDA antagonists (bicuculline and D-APV). The effects of N129–164 infusion were recorded after 30–40 min. For details, see Supplementary data.

Supplementary data

Supplementary data are available at *The EMBO Journal* Online.

Acknowledgements

We acknowledge the excellent technical assistance of Liliane Glauser, Sarah Magnin and Marlis Moosmayer. We thank Drs R Luthi-Carter, C Lebrand and C Petersen for critical reading of the manuscript. This work was supported by grants from the Swiss National Science Foundation (no. 3100AO-100834/1) and from the Leenaards Foundation (1907/ep).

References

Alberi S, Boda B, Steiner P, Nikonenko I, Hirling H, Muller D (2005) The endosomal protein NEEP21 regulates AMAP receptor-mediated synaptic transmission and plasticity in the hippocampus. *Mol Cell Neurosci* **29:** 313–319

Barry MF, Ziff EB (2002) Receptor trafficking and the plasticity of excitatory synapses. *Curr Opin Neurobiol* **12:** 279–286

Beattie EC, Carroll RC, Yu X, Morishita W, Yasuda H, von Zastrow M, Malenka RC (2000) Regulation of AMPA receptor endocytosis by a signaling mechansim shared with LTD. *Nat Neurosci* **3:** 1291–1300

Blaschke M, Keller BU, Rivosecchi R, Hollmann M, Heinemann S, Konnerth A (1993) A single amino acid determines the subunit-specific spider toxin block of alpha-amino-3-hydroxy-5-methylisoxazole-4-propionate/kainate receptor channels. *Proc Natl Acad Sci USA* **90:** 6528–6532

Braithwaite SP, Xia H, Malenka RC (2002) Differential roles for NSF and GRIP/ABP in AMPA receptor cycling. *Proc Natl Acad Sci USA* **99:** 7096–7101

Bredt DS, Nicoll RA (2003) AMPA receptor trafficking at excitatory synapses. *Neuron* **40:** 361–379

Chung HJ, Xia J, Scannevin RH, Zhang X, Huganir RL (2000) Phosphorylation of the AMPA receptor subunit GluR2 differentially regulates its interaction with PDZ domain-containing proteins. *J Neurosci* **20:** 7258–7267

Collingridge GL, Isaac JT (2003) Functional roles of protein interactions with AMPA and kainate receptors. *Neurosci Res* **47:** 3–15

Daw MI, Chittajallu R, Bortolotto ZA, Dev KK, Duprat F, Henley JM, Collingridge GL, Isaac JT (2000) PDZ proteins interacting with C-terminal GluR2/3 are involved in a PKC-dependent regulation of AMPA receptors at hippocampal synapses. *Neuron* **28:** 873–886

Debaigt C, Hirling H, Steiner P, Vincent JP, Mazella J (2004) Crucial role of neuron-enriched endosomal protein of 21 kD in sorting between degradation and recycling of internalized G protein-coupled receptors. *J Biol Chem* **279:** 35687–35691

Dong H, O'Brien RJ, Fung ET, Lanahan AA, Worley PF, Huganir RL (1997) GRIP: a synaptic PDZ domain-containing protein that interacts with AMPA receptors. *Nature* **386:** 279–284

Ehlers MD (2000) Reinsertion or degradation of AMPA receptors determined by activity-dependent endocytic sorting. *Neuron* **28:** 511–525

Feng W, Fan JS, Jiang M, Shi YW, Zhang M (2002) PDZ7 of glutamate receptor interacting protein binds to its target via a novel hydrophobic surface area. *J Biol Chem* **277:** 41140–41146

Florin EL, Moy VT, Gaub HE (1994) Adhesion forces between individual ligand–receptor pairs. *Science* **264:** 415–417

Gage RM, Matveeva EA, Whiteheart SW, von Zastrow M (2005) Type I PDZ ligands are sufficient to promote rapid recycling of G protein-coupled receptors independent of binding to *N*-ethylmaleimide-sensitive factor. *J Biol Chem* **280:** 3305–3313

Heynen AJ, Yoon BJ, Liu CH, Chung HJ, Huganir RL, Bear MF (2003) Molecular mechanism for loss of visual cortical responsiveness following brief monocular deprivation. *Nat Neurosci* **6:** 854–862

Hirling H, Steiner P, Chaperon C, Marsault R, Regazzi R, Catsicas S (2000) Syntaxin 13 is a developmentally regulated SNARE involved in neurite outgrowth and endosomal trafficking. *Eur J Neurosci* **12:** 1913–1923

Hollmann M, Hartley M, Heinemann S (1991) Ca^{2+} permeability of KA-AMPA-gated glutamate receptor channels depends on subunit composition. *Science* **252:** 851–853

Lee SH, Simonetta A, Sheng M (2004) Subunit rules governing the sorting of internalized AMPA receptors in hippocampal neurons. *Neuron* **43:** 221–236

Lin JW, William J, Foster K, Lee SH, Ahmadian G, Wyszynski M, Wang YT, Sheng M (2000) Distinct molecular mechanisms and divergent endocytotic pathways of AMPA receptor internalization. *Nat Neurosci* **3:** 1282–1290

Liu S, Lau L, Wei J, Zhu D, Zou S, Sun HS, Fu Y, Liu F, Lu Y (2004) Expression of Ca(2+)-permeable AMPA receptor channels primes cell death in transient forebrain ischemia. *Neuron* **43:** 43–55

Lu HC, She WC, Plas DT, Neumann PE, Janz R, Crair MC (2003) Adenylyl cyclase I regulates AMPA receptor trafficking during mouse cortical 'barrel' map development. *Nat Neurosci* **6:** 939–947

Lu WY, Man HY, Ju W, Trimble WS, Macdonald JF, Wang YT (2001) Activation of synaptic NMDA receptors induces membrane insertion of new AMPA receptors and LTP in cultured hippocampal neurons. *Neuron* **29:** 243–254

Luscher C, Xia H, Beattie EC, Carroll RC, von Zastrow M, Malenka RC, Nicoll RA (1999) Role of AMPA receptor cycling in synaptic transmission and plasticity. *Neuron* **24:** 649–658

Malinow R, Malenka RC (2002) AMPA receptor trafficking and synaptic plasticity. *Annu Rev Neurosci* **25:** 103–126

Man HY, Lin JW, Ju WH, Ahmadian G, Liu LD, Becker LE, Sheng M, Wang YT (2000) Regulation of AMPA receptor-mediated synaptic transmission by clathrin-dependent receptor internalization. *Neuron* **25:** 649–662

Matsuda S, Launey T, Mikawa S, Hirai H (2000) Disruption of AMPA receptor GluR2 clusters following long-term depression induction in cerebellar Purkinje neurons. *EMBO J* **19:** 2765–2774

Maxfield FR, McGraw TE (2004) Endocytic recycling. *Nat Rev Mol Cell Biol* **5:** 121–132

McBride HM, Rybin V, Murphy C, Giner A, Teasdale R, Zerial M (1999) Oligomeric complexes link Rab5 effectors with NSF and drive membrane fusion via interactions between EEA1 and syntaxin 13. *Cell* **98:** 377–386

Muller BM, Kistner U, Veh RW, Cases-Langhoff C, Becker B, Gundelfinger ED, Garner CC (1995) Molecular characterization and spatial distribution of SAP97, a novel presynaptic protein homologous to SAP90 and the *Drosophila* discs-large tumor suppressor protein. *J Neurosci* **15:** 2354–2366

Noel J, Ralph GS, Pickard L, Williams J, Molnar E, Uney JB, Collingridge GL, Henley JM (1999) Surface expression of AMPA receptors in hippocampal neurons is regulated by an NSF-dependent mechanism. *Neuron* **23:** 365–376

Passafaro M, Piech V, Sheng M (2001) Subunit-specific temporal and spatial patterns of AMPA receptor exocytosis in hippocampal neurons. *Nat Neurosci* **4:** 917–926

Pellegrini-Giampietro DE, Gorter JA, Bennett MV, Zukin RS (1997) The GluR2 (GluR-B) hypothesis: Ca(2+)-permeable AMPA receptors in neurological disorders. *Trends Neurosci* **20:** 464–470

Prekeris R, Klumperman J, Chen YA, Scheller RH (1998) Syntaxin 13 mediates cycling of plasma membrane proteins via tubulovesicular recycling endosomes. *J Cell Biol* **143:** 957–971

Sheng M, Kim MJ (2002) Postsynaptic signaling and plasticity mechanisms. *Science* **298:** 776–780

Shi SH, Hayashi Y, Esteban JA, Malinow R (2001) Subunit-specific rules governing AMPA receptor trafficking to synapses in hippocampal pyramidal neurons. *Cell* **105:** 331–343

Shi SH, Hayashi Y, Petralia RS, Zaman SH, Wenthold RJ, Svoboda K, Malinow R (1999) Rapid spine delivery and redistribution of AMPA receptors after synaptic NMDA receptor activation. *Science* **284:** 1811–1816

Song I, Huganir RL (2002) Regulation of AMPA receptors during synaptic plasticity. *Trends Neurosci* **25:** 578

Song I, Kamboj S, Xia J, Dong H, Liao D, Huganir RL (1998) Interaction of the *N*-ethylmaleimide-sensitive factor with AMPA receptors. *Neuron* **21:** 393–400

Steiner P, Sarria JC, Glauser L, Magnin S, Catsicas S, Hirling H (2002) Modulation of receptor cycling by neuron-enriched endosomal protein of 21 kD. *J Cell Biol* **157:** 1197–1209

Stoppini L, Buchs PA, Muller D (1991) A simple method for organotypic cultures of nervous tissue. *J Neurosci Methods* **37:** 173–182

Takahashi T, Svoboda K, Malinow R (2003) Experience strengthening transmission by driving AMPA receptors into synapses. *Science* **299:** 1585–1588

Terashima A, Cotton L, Dev KK, Meyer G, Zaman S, Duprat F, Henley JM, Collingridge GL, Isaac JT (2004) Regulation of synaptic strength and AMPA receptor subunit composition by PICK1. *J Neurosci* **24:** 5381–5390

Turrigiano GG, Nelson SB (2004) Homeostatic plasticity in the developing nervous system. *Nat Rev Neurosci* **5:** 97–107

Xia J, Chung HJ, Wihler C, Huganir RL, Linden DJ (2000) Cerebellar long-term depression requires PKC-regulated interactions between GluR2/3 and PDZ domain-containing proteins. *Neuron* **28:** 499–510

Yersin A, Hirling H, Steiner P, Magnin S, Regazzi R, Huni B, Huguenot P, De Los Rios P, Dietler G, Catsicas S, Kasas S (2003) Interactions between synaptic vesicle fusion proteins explored by atomic force microscopy. *Proc Natl Acad Sci USA* **100:** 8736–8741

